

# Effects of pre-processing on reverse time migration: a North Sea study

Ian F. Jones\*

## Abstract

Almost all conventional pre-processing is conceived with one-way wave propagation in mind. If we take into account the existence of events arising from two-way wave propagation, then many of the underlying assumptions of moveout behaviour implicit in some pre-processing techniques must be re-evaluated. Using 2D synthetic data, we demonstrate that the moveout behaviour of double bounce arrivals (a class of two-way propagating events) can be compromised by pre-processing designed to remove events exhibiting 'anomalous' moveout behaviour. These observations are of interest to us because we are now beginning to employ two-way migration schemes to image complex structures. However, if we continue to use conventional pre-processing techniques, we run the risk of removing the very events we are trying to image. The observations made on the basis of synthetic modelled data are extended in this work to real data examples, all from the North Sea, where in the Central Graben we commonly have steep-sided salt diapir piercements, which are good candidates for producing useful double bounce arrivals that can be imaged using reverse time migration.

## Introduction

The speed and cost effectiveness of contemporary computer systems now permit us to implement more general algorithmic solutions of the wave equation (Whitmore, 1983; Baysal et al., 1983; McMechan, 1984; Bednar et al., 2003; Yoon et al., 2003; Shan & Biondi, 2004; Zhou et al., 2006; Zhang et al., 2006). The restriction to one-way propagation can be lifted, and data migrated to take advantage of more esoteric propagation paths, such as turned rays, double bounce arrivals and, potentially, multiples (Mittet, 2006). However, in order to take advantage of these improved algorithms, we must ensure that the data input to migration have not been compromised in any way. Specifically, in this work we address the moveout behaviour of double bounce events (Hawkins et al., 1995; Bernitsas et al., 1997; Cavalca & Lailly, 2005), and note how many conventional pre-processing algorithms can damage these arrivals, thus rendering some aspects of any subsequent high-end migration superfluous.

We commence our analysis by reviewing the conclusions of preliminary work on synthetic data (Jones, 2008, *in prep*) which discussed the moveout behaviour of turning waves (Hale et al., 1992) and simple double bounce events (also referred to as 'prism waves' by some authors). For ease of demonstration, we firstly employ a ray-tracing package, with which we can model individual selected arrivals, and later create more complex synthetic data using an elastic finite difference (FD) package. Some brief details of these packages are given.

After investigating the moveout behaviour of the simple models, we move on to a model representing a complex North Sea salt dome structure (Davison et al., 2000; Thomson, 2004; Farmer et al., 2006). We show the effect of various

conventional pre-processing steps on double bounce arrivals, and carry these analyses through to migration with a 2D reverse time migration (RTM) algorithm capable of imaging the double bounce arrivals. We then extend this analysis and demonstration on 2D synthetic data to real data, where we see similar classes of event and the same degradation of double bounce arrivals shown in the synthetic trials.

## Work programme

Using a workstation-based 2D modelling system, we generated acoustic ray-traced CMP data as a control to identify various individual arrivals. The initial data creation and analysis were performed for simple geometries, and then repeated for a complex North Sea salt diapir model (2 ms sampling, peak-frequency ~35 Hz, shot interval 50 m, CMP interval 6.25 m, 6 km maximum offset).

We then generated more 'realistic' elastic FD shot gather data for the complex North Sea salt diapir model. These modelled data included attenuation with an absorbing boundary condition, using the same vertical interval velocity model as the ray-traced model for 1 ms data (resampled to 4 ms for processing), and a peak-frequency of ~17 Hz. In this study we have used an absorbing surface boundary; hence the FD data contain no free-surface multiples (whereas the ray-trace data do). The explicit 2D/3D elastic wave propagation code is 4th-order accurate in space and 2nd-order accurate in time, and is based on the elastodynamic formulation of the wave equation on a staggered grid (Madariaga, 1976; Virieux, 1986; Levander, 1988; Larsen & Grieger, 1998).

We pre-processed the FD data using 'conventional' data processing flows that are likely to damage double bounce events, including:

\* ION GX Technology EAME, 180 High Street, Egham, Surrey TW20 9DY, UK.  
E-mail: ian.jones@iongeo.com.

- Tau-P mute for backscattered noise
- Radon demultiple
- CMP domain apex-shifted multiple attenuation (ASMA)

After each pre-processing flow, we applied 2D RTM and assessed the preservation of double bounce (prism wave) arrivals in the resultant images. In all cases, the direct arrival was muted on the data input to the RTM process.

**The modelling**

We commence by looking at three simple scenarios:

- A simple right-angle corner reflector
- An acute angle reflector (non-crossing rays)
- An acute angle reflector (crossing rays)

With this layout, there are no double bounce arrivals for an obtuse angle geometry: we would need extremely long offsets and large arrival times.

These three scenarios are shown in Figure 1. It is clear that the moveout behaviour does not conform to what we

expect for normal-incidence raypaths that can be migrated with a one-way algorithm, but more closely resembles events such as those resulting from scattered energy or diffracted multiples. We know that for simple quasi-1D cylindrical models all co-axially recorded events in a CMP gather will appear with their apex at zero offset. It is this observation that guides the design principle of various multiple suppression techniques and provides the justification for muting in Tau-P space to suppress backscattered energy.

We now look at a full synthetic data set created along a 2D crestal line of the 3D production model representing our North Sea example, and show the effects of various pre-processing techniques on these data. For the geometry in Figure 2, we have:

- A single bounce at the flat-lying part of a reflector
- A single bounce at the dipping part of this reflector
- A non-crossing double bounce involving the flat and dipping reflectors
- A crossing double bounce involving the flat and dipping reflectors (not shown to avoid clutter)

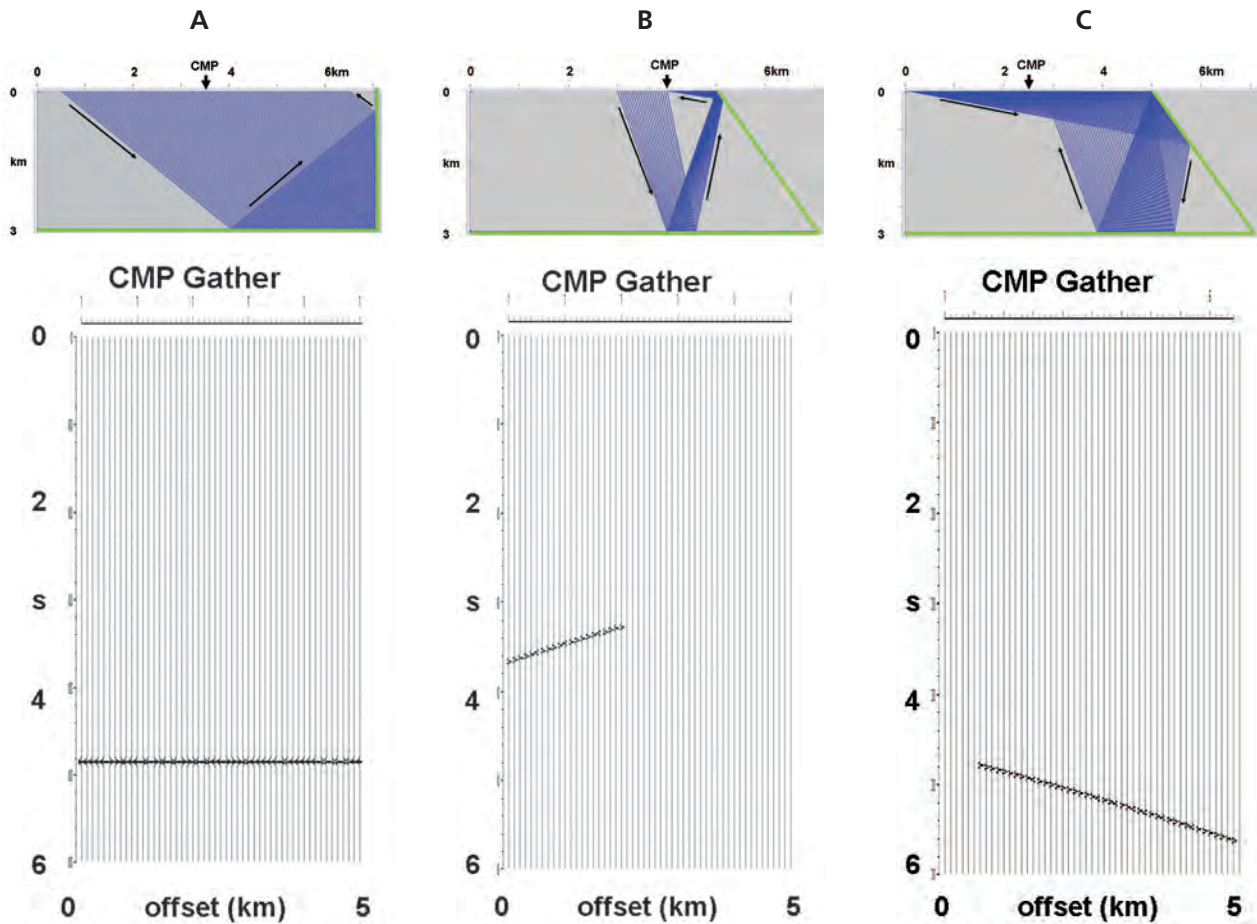


**Figure 1** In each example, the model horizons are shown in green and arrows indicate the propagation direction on the sample ray paths. The resulting CMP gather is shown below each frame. (a) Right-angle corner reflector travel time is constant with offset: i.e. no moveout. (b) Acute angle, non-crossing events. Arrivals are only present on the near offsets, and arrival time decreases with offset. (c) Acute angle, crossing events. Arrivals are present on most offsets, and arrival time increases with offset.

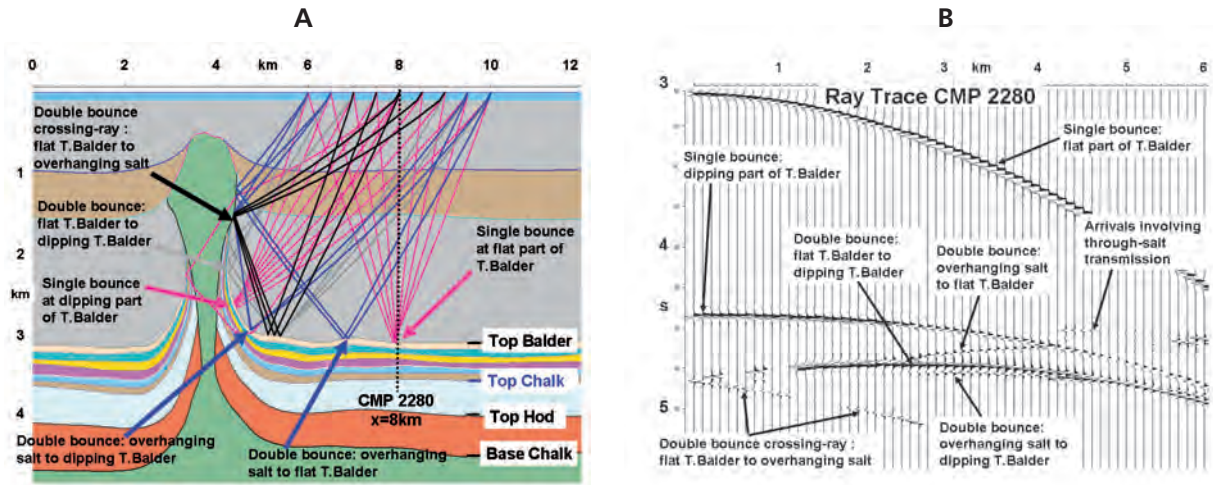


Figure 2 (a) Plot of a few sparse rays shown against the interval velocity model. The sediment velocity ranges from about 1900 m s<sup>-1</sup> to 2200 m s<sup>-1</sup>, with some shallow impedance contrast events. The absence of a strong sediment gradient precludes turning rays in the sediments, although a strong compaction velocity gradient below the Top Balder and Top Chalk does produce turning rays. The salt velocity (green) is 4500 m s<sup>-1</sup> and the Chalk velocity is between 5500 m s<sup>-1</sup> and 6000 m s<sup>-1</sup>. (b) A single CMP gather from the surface location at 8 km.

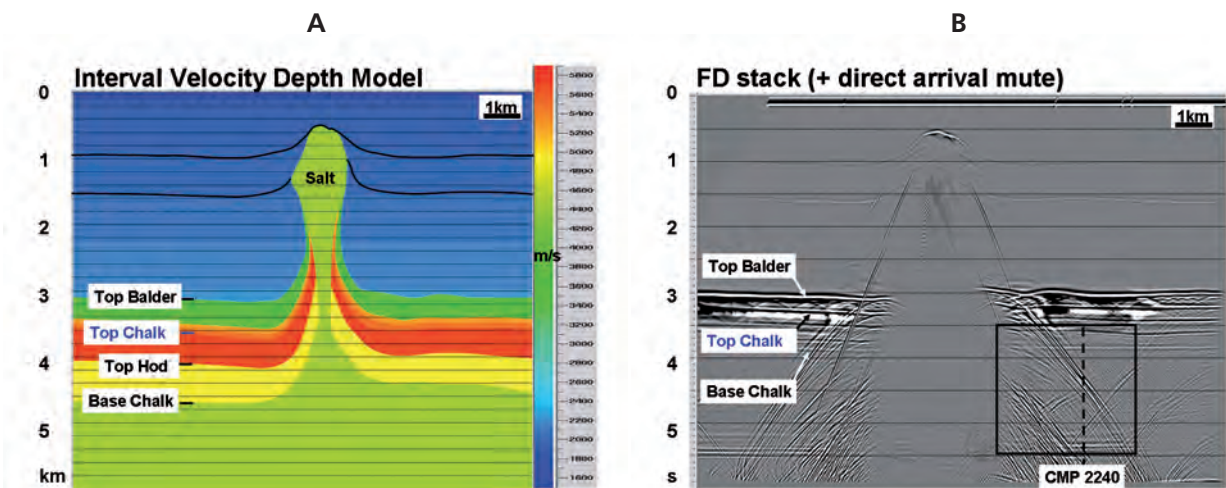


Figure 3 (a) The velocity depth model, with main horizons indicated. (b) The brute stack of the FD data. The direct arrivals have been muted.

- Raypaths passing into the salt with an internal reflection at the steep salt wall and a second bounce outside the salt from the flat or steep reflectors (which are not considered here as they have relatively low amplitude due to the transmission coefficients at the salt wall)

The velocity model is based on a 2D crestal line taken from an actual 3D North Sea example (Farmer et al., 2006). The production project in that case was anisotropic, using VTI 3D RTM code, but for simplicity here we are using 2D isotropic modelling and 2D isotropic RTM.

From the ray-tracing exercises, we can clearly see which are the single and which are the double bounce events illuminating the salt flank. We can also identify a class of events passing through the salt body itself and illuminating the salt flank, but these are weak due to the impedance contrast at the salt boundary and will not be discussed here. Figure 3

shows the interval velocity model and associated elastic FD stack. No velocity analysis was carried out. The stack was produced using the RMS velocity function associated with the interval velocity model, and the direct arrival has been muted out.

Figure 4 shows an enlargement of the diffraction tails on the right flank of the dome from Figure 3b. We see the ray-trace modelling with and without double bounce events, permitting us to identify where they occur in the section. Also shown is the full elastic FD result. These differences can be seen more clearly in an individual CMP gather. Figure 5 shows a gather at CMP location 2240, for ray-tracing including double bounces, and full elastic FD modelling. It is clear here why it is necessary to perform ray-trace modelling for individual sets of events: without ray-trace modelling, it is too difficult to understand what we are seeing in the FD data.

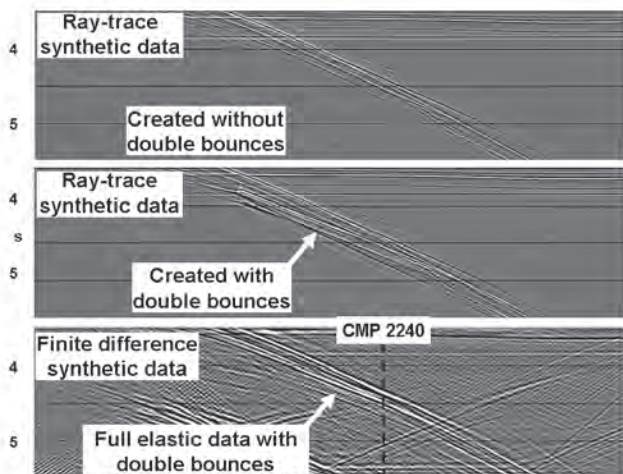


Figure 4 Detail of CMP stacked sections for the ray-traced synthetic data as well as the FD data from box indicated in Figure 3b, showing location of double bounce events in diffraction tails. Also noted is the location of CMP 2240.

### Pre-processing

Essentially, we are looking at processes that eliminate events which exhibit anomalous moveout behaviour in the CMP domain. For conventional 2D geometry, in a one-way wave propagation paradigm, such events constitute diffracted multiples and scattered energy. In other words, they are events that appear to have secondary source locations from a one-way perspective. In reality, these events are examples of two-way wave propagation, in that the raypath changes direction before or after its ‘main’ reflection from the interface of interest.

We began by assessing Radon demultiple. If we were to employ the Radon filter to directly output the multiple-free ‘primaries’, then we would have a problem because all apex-shifted events would be corrupted, appearing as smeared artefacts in the output. However, this issue can be circumvented if we use the Radon to model the multiples, and then adaptively

subtract them from the input data. Working in this way, we would preserve the apex-shifted arrivals in the CMP gather. Consequently, we do not show the Radon results here.

We then assessed an apex-shifted multiple attenuation routine (ASMA), designed to attenuate events whose apexes are shifted from zero offset in CMP gathers, as a first order approximation to 3D SRME. By design, this effectively eradicates the double bounce events.

Lastly, we assessed a Tau-P mute (for backscattered noise). Normally, this is performed in conjunction with a deconvolution. Here we have not applied the deconvolution step in order to isolate and highlight the effect of the Tau-P mute. Also, because we used an absorbing surface boundary condition in the FD modelling, the short-period water bottom multiples are not present in the elastic 3D modelled data.

We show the effects of these processing sequences for a set of CMP gathers straddling the salt dome. Figure 6 shows the raw input FD modelled data and the outputs from ASMA, Tau-P muting, and both these processes. Apex-shifted events have been attenuated. This would be considered a good thing for conventional processing, but is deleterious for two-way imaging.

### Effects on RTM migration

Figure 7a shows the RTM of the FD raw data using a slightly smoothed model, and post-processing to enhance the image. However, in an industrial flow, where we are trying to determine the model, we would approach the definition of the salt flank using a migration with a salt-free model. In RTM, the imaging condition will still produce an image of the salt flank from double bounce events as long as the flat-lying layers of high velocity contrast are present in the model. So, in order to evaluate the effect of our pre-processing on the imaging of the double bounce arrivals, we compare results using RTM with a no-salt model. Figure 7b shows the image of the raw data with

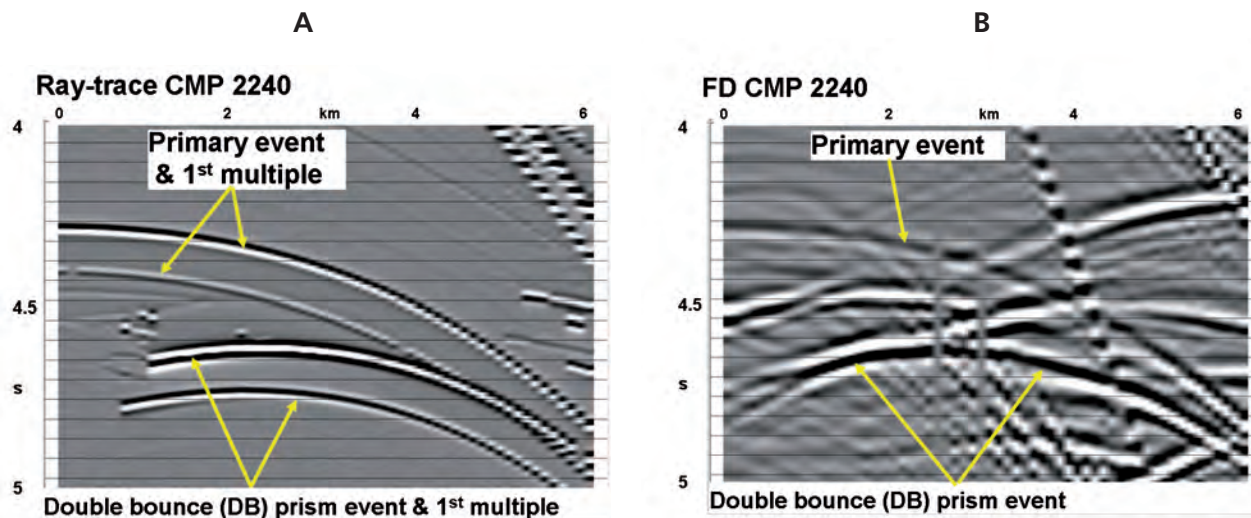


Figure 5 (a) A CMP (model location 2240) for the acoustic ray-traced data with double bounces, including the free-surface multiple. (b) The elastic FD data, without free-surface multiples.

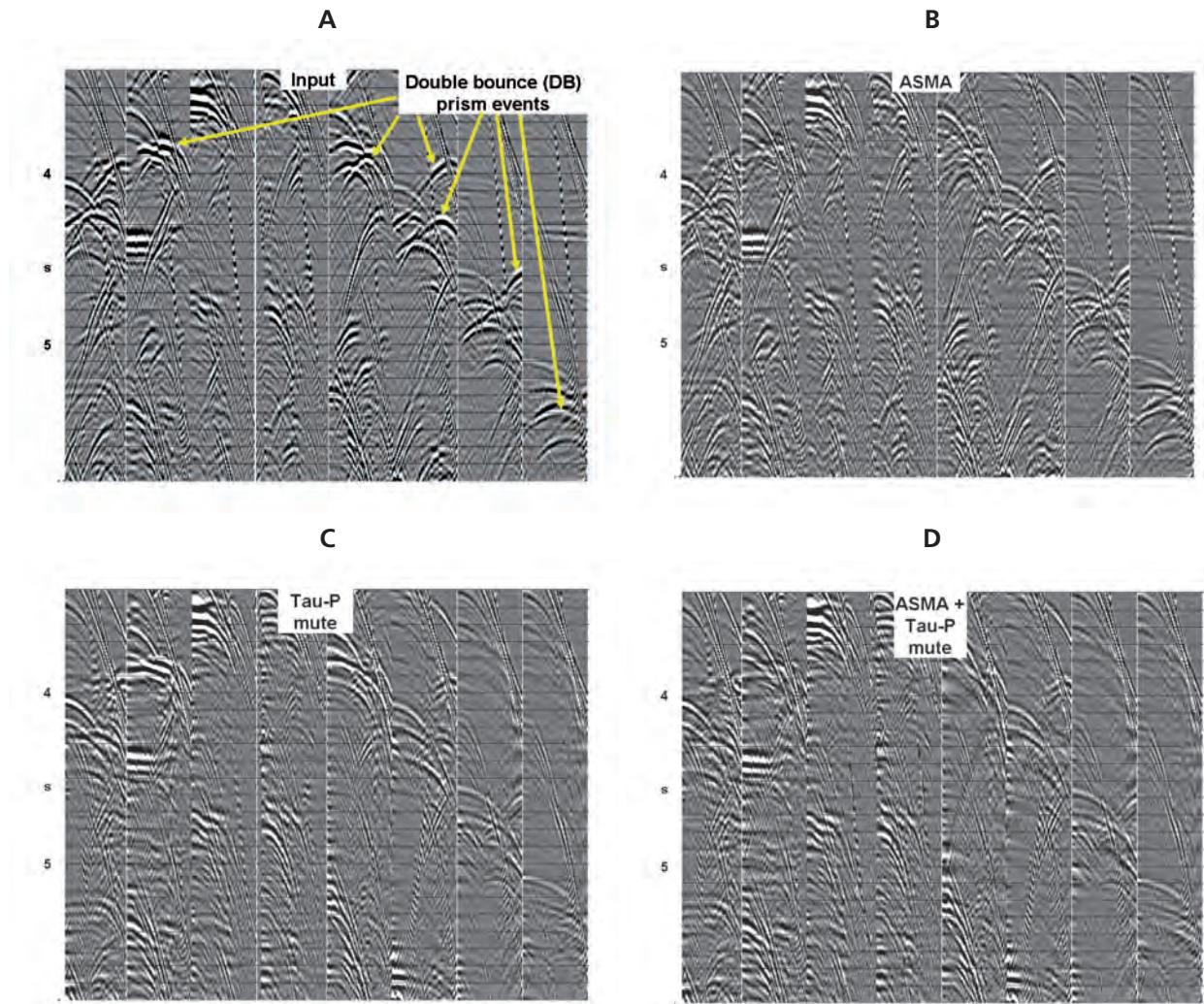


Figure 6 (a) Selection of gathers with 6 km maximum offset from the FD modelled data, showing the raw input. Outputs from (b) ASMA which has performed slightly better than Tau-P on the left of the section, (c) Tau-P muting which has performed better on the right, and (d) both these processes.

the no-salt model. In both parts of Figure 7 the interval velocity model used in the migration is superimposed. Figure 8a shows the RTM image of Figure 7 without the colour model overlay, and Figure 8b shows the RTM image using the no-salt model of the data subjected to Tau-P mute and ASMA. It is clear that the vertical and overturned salt-flank events have been seriously attenuated in the latter sequence.

**Real data**

Having demonstrated the deleterious effects of inappropriate pre-processing on RTM imaging using the synthetic data, we now consider a real North Sea example. In fact it was the mixed success of RTM migration on such salt structures that alerted us to the issues described here. On one project (Farmer et al., 2006) the results were impressive. However, on a subsequent project involving a neighbouring salt dome with similar geology and similar acquisition, the results of RTM were disappointing in part, perhaps, due to model inaccuracies, but possibly also due to the effects of slightly different pre-processing.

Here we have revisited the successful project and re-worked the pre-processing to attempt to assess the damage done by typical production pre-processing. In the production project mentioned, conducted in 2005–2006, serendipitously no deleterious pre-processing was applied. In the unsuccessful project, a Tau-P mute was used to attenuate problematic back-scattered noise. Here we have taken this same Tau-P mute and applied it to data from the first (successful) project. The tests have been conducted only in 2D, using a crestal line, but the conclusions are valid for the 3D case.

Figure 9 shows the input data along the selected crestal line and the anisotropic 3D RTM of these data with an intermediate (no-salt) model, highlighting the double bounce events (Farmer et al., 2006).

The input CMP gathers, with maximum offset 3100 m, as used in the successful production project (and to make the stack shown in Figure 9a) are shown in Figure 10a. The effect of applying a Tau-P mute, designed to remove ‘backscattered’ energy, is shown in Figure 10b. In this case, we note that it damages

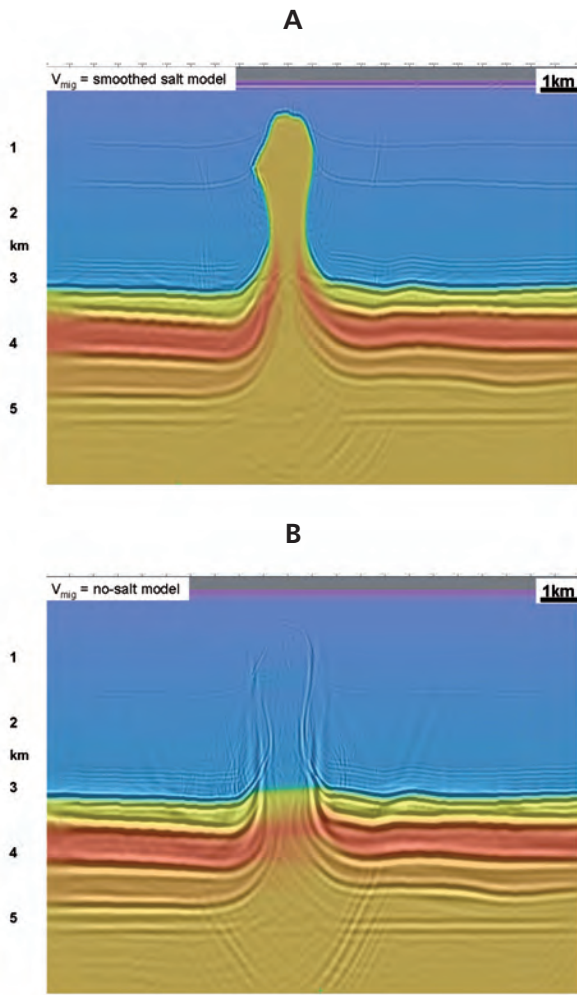


Figure 7 (a) RTM with raw data and salt model. (b) RTM with raw data and no-salt model. The salt wall image looks nicer in the no-salt model as we avoid the (correct) model-imposed wavelet stretch at the salt boundary. The imaging condition still constructs the salt wall event, as we have one bounce point specified in the model (the flat-lying Top Balder).

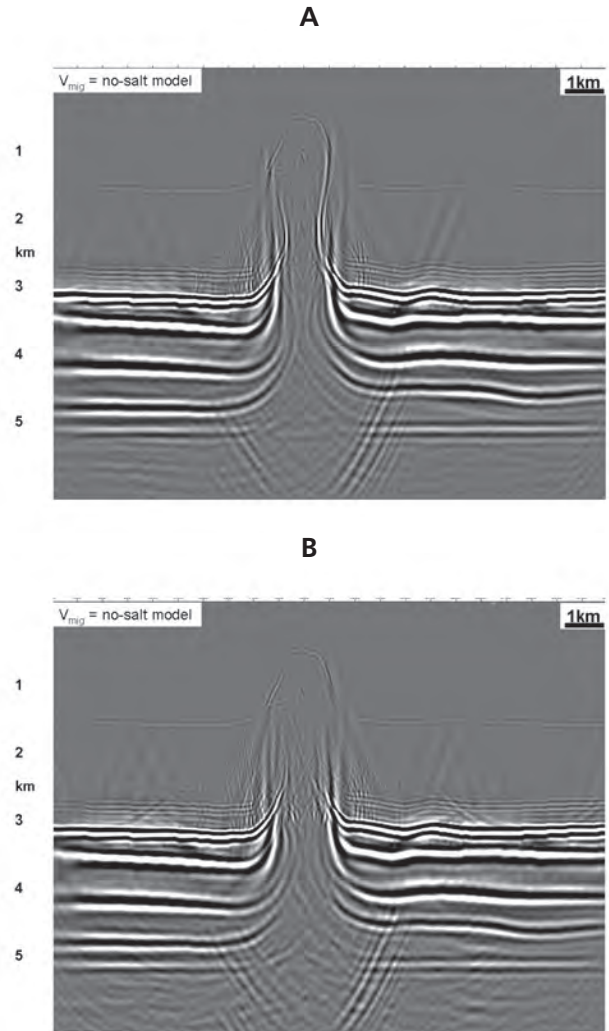


Figure 8 RTM images of (a) the raw data and (b) the data processed with ASMA and Tau-P muting. The overturned salt wall reflectors have been significantly damaged by this conventional pre-processing flow.

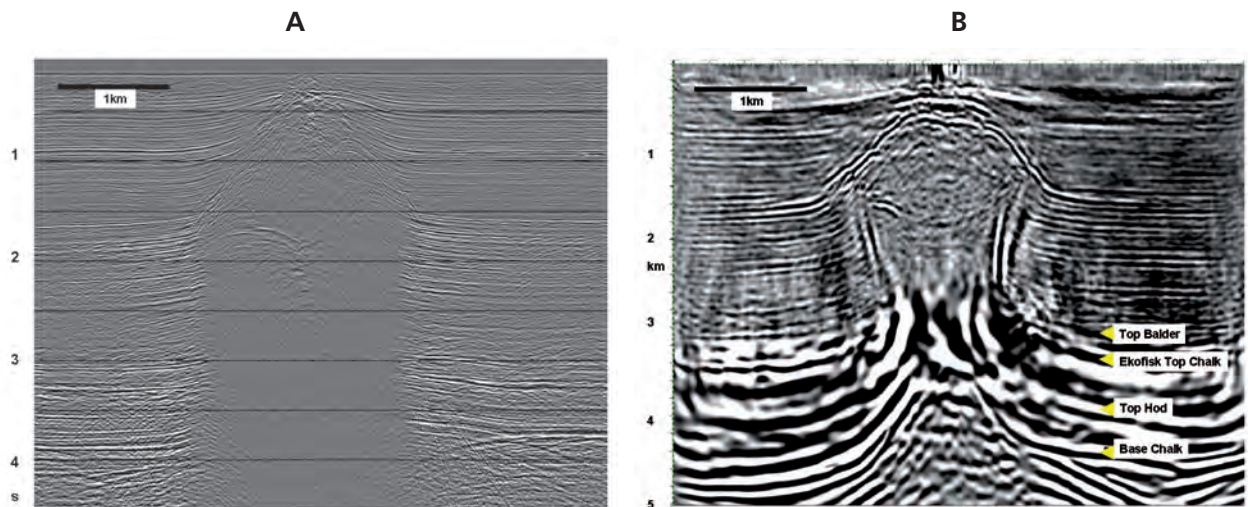
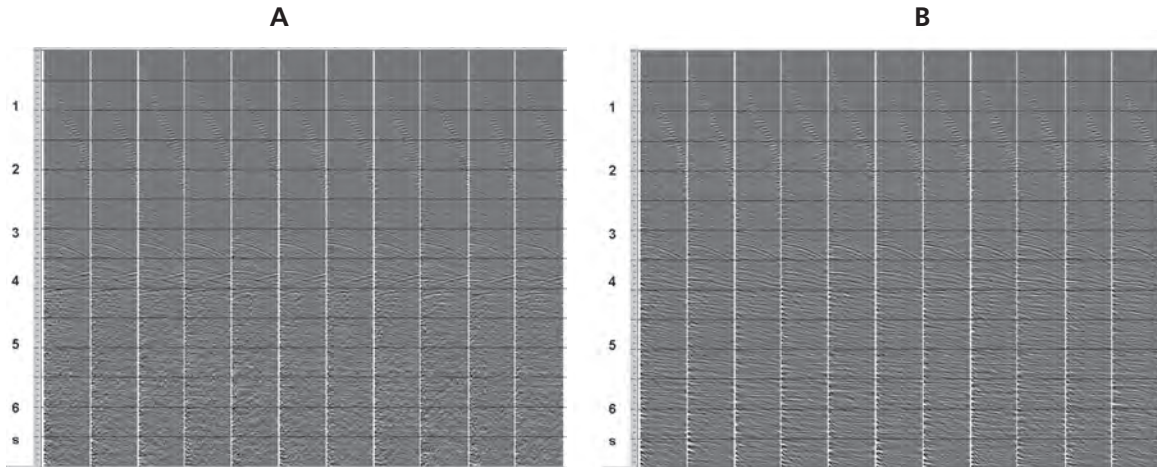
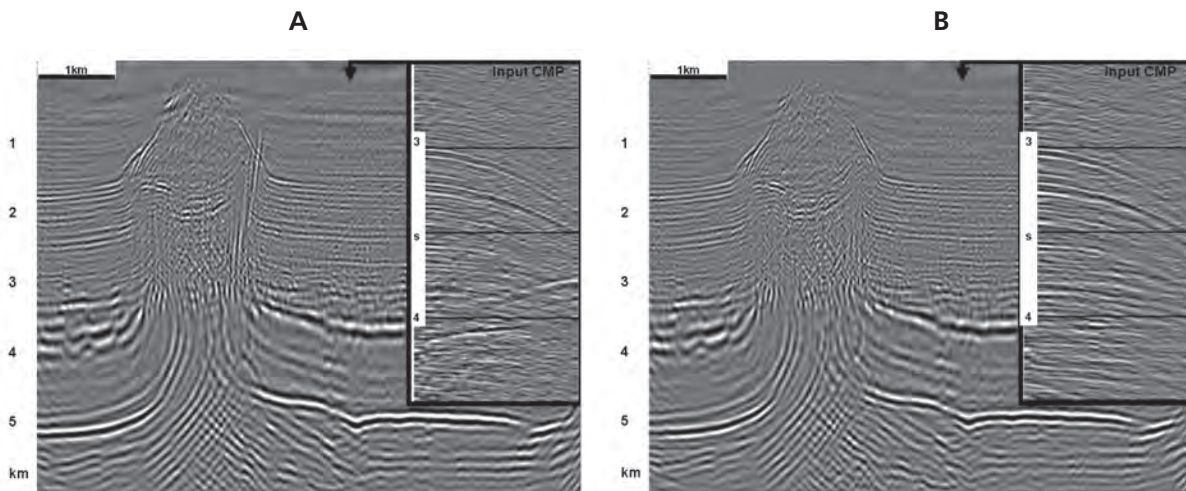


Figure 9 (a) Stack of CMP gathers input to the successful project. (b) Intermediate anisotropic 3D RTM result with a no-salt model.



**Figure 10** (a) CMP gathers (with maximum offset 3100 m) input to the successful project. (b) CMP gathers after application of a Tau-P domain mute designed to attenuate back-scattered energy (thus affecting apex-shifted CMP events). The contra-dipping events have been suppressed. These are suspected to be double bounce arrivals.



**Figure 11** (a) Isotropic 2D RTM of SRME data using a no-salt model. We see double bounce energy arrivals appearing as near-vertical events in the vicinity of the salt flanks. (b) RTM with the same model, but using as input the data after the Tau-P mute. The double bounce energy has been removed. The insets are individual CMP gathers showing the double bounce events which are removed by the Tau-P mute.

events with shifted apices. From the perspective of conventional processing, this result would normally be considered good, but as we now know, it will prove damaging to RTM.

Figure 11a shows the 2D RTM of SRME data using a no salt model. We see double bounce energy arrivals appearing as near-vertical events in the vicinity of the salt flanks. Figure 11b shows the RTM image with the same model, but using as input the data after the Tau-P mute. The double bounce energy has been removed. In each part of the figure, there is an inset of a CMP gather showing the data going into the migration. It is evident that double bounce events are removed by the Tau-P mute, as they resemble back-scattered energy, appearing with a shifted apex in the CMP domain.

**Conclusions**

Conventional pre-processing is designed to remove various classes of noise, such as backscattered energy, multiples, and

diffracted multiples. The processes designed to do this have, for the most part, been designed with one-way wave propagation of primary energy in mind.

Software developers have spent several years developing these routines that will efficiently remove diffracted multiples and back-scattered noise, developing the apex-shifted approach and more recently 3D SRME. However, if we set out to migrate two-way propagated primary energy, as is now possible with the new generation of migration algorithms such as RTM, we need to ensure that our pre-processing flow is fit-for-purpose and does not inadvertently damage the very events we are trying to image.

Typically, two-way propagated primary events, such as double bounces, appear in the CMP domain with their moveout apex-shifted from zero offset. As such, they resemble diffracted multiples or backscattered energy. Consequently, tools such as 3D SRME must be employed,

instead of more conventional 2D approaches, to suppress multiples in complex environments to avoid unnecessary removal of useful primary (two-way) energy.

### Acknowledgements

The workstation-based 2D modelling system used here (GXII) was developed by Don Larson at GX Technology. I thank Mike Goodwin, Stuart Greenwood, and Brent Mecham for help to create the synthetic data, and Dave King, Mick Sugrue, and Ivan Berranger for discussions and help with the RTM jobs. I also thank the management of ION GX Technology for permission to publish the results of this study.

### References

- Baysal, E., Kosloff, D.D. and Sherwood, J.W.C. [1983] Reverse time migration. *Geophysics*, 48, 1514-1524.
- Bednar, J.B., Yoon, K., Shin, C. and Lines, L.R. [2003] One way vs two way wave equation imaging – is two-way worth it? *65<sup>th</sup> EAGE Conference and Exhibition*, Extended Abstracts, B011.
- Bernitsas, N., Sun, J. and Sicking, C. [1997] Prism waves – an explanation for curved seismic horizons below the edge of salt bodies. *59<sup>th</sup> EAGE Conference and Exhibition*, Extended Abstracts, E038.
- Cavalca, M. and Lailly, P. [2005] Prismatic reflections for the delineation of salt bodies. *75<sup>th</sup> SEG Annual International Meeting*, Expanded Abstracts, 2550-2553.
- Davison, I., Alsop, G.I., Evans, N.G. and Safaricz, M. [2000] Overburden deformation patterns and mechanisms of salt diapir penetration in the Central Graben, North Sea. *Marine and Petroleum Geology*, 17, 601-618.
- Farmer, P., Jones, I.F., Zhou, H., Bloor, R. and Goodwin, M.C. [2006] Application of reverse time migration to complex imaging problems. *First Break*, 24(9), 65-73.
- Hale, D., Hill, N.R. and J. Stefani [1992] Imaging salt with turning seismic waves. *Geophysics*, 57, 1453-1462.
- Hawkins, K., Cheng, C.-C., Sadek, S.A. and Brzostowski, M.A. [1995] A v(z) DMO developed with the North Sea Central Graben in mind. *65<sup>th</sup> SEG Annual International Meeting*, Expanded Abstracts, 1429-1432.
- Jones, I.F. [2008] A modeling study of pre-processing considerations for reverse time migration, *Geophysics*, (in prep).
- Larsen, S.C. and Grieger, J.C. [1998] Elastic modeling initiative, Part III: 3-D computational modeling. *68<sup>th</sup> SEG Annual International Meeting*, Expanded Abstracts, 1803-1806.
- Levander, A.R. [1988] Fourth-order finite-difference P-SV seismograms. *Geophysics*, 53, 1425-1436.
- Madariaga R. [1976] Dynamics of an expanding circular fault. *Bulletin of the Seismological Society of America*, 66, 639-666.
- McMechan, G.A. [1983] Migration by extrapolation of time-dependent boundary values. *Geophysical Prospecting*, 31, 413-420.
- Mitter, R. [2006]. The behaviour of multiples in reverse time migration. *68<sup>th</sup> EAGE Conference and Exhibition*, Workshop 6.
- Shan, G. and Biondi, B. [2004] Imaging overturned waves by plane wave migration in tilted co-ordinates. *74<sup>th</sup> SEG Annual International Meeting*, Expanded Abstracts, 969-972.
- Thomson, K. [2004] Overburden deformation associated with halokinesis in the Southern North Sea: implications for the origin of the Silverpit Crater. *Visual Geosciences*, 9, 1-9.
- Virieux, J. [1986] P-SV wave propagation in heterogeneous media – velocity-stress finite-difference method. *Geophysics*, 51, 889-901.
- Whitmore, N.D. [1983] Iterative depth migration by backward time propagation. *53<sup>rd</sup> SEG Annual International Meeting*, Expanded Abstracts, 382-385.
- Yoon, K., Shin, C., Suh, S., Lines, L.R. and Hong, S. [2003] 3D reverse-time migration using the acoustic wave equation: an experience with the SEG/EAGE data set. *The Leading Edge*, 22(1), 38-41.
- Zhou, H., Zhang, G. and Bloor, R. [2006] An anisotropic acoustic wave equation for VTI Media. *68<sup>th</sup> EAGE Conference and Exhibition*, Extended Abstracts, H033.
- Zhang, Y., Sheng, X. and Zhang, G. [2006] Imaging complex salt bodies with turning-wave one-way wave equation. *SEG/EAGE Summer Research Workshop, Utah*.

Received 28 November 2007; accepted 25 February 2008.



**EAGE**  
EUROPEAN  
ASSOCIATION OF  
GEOSCIENTISTS &  
ENGINEERS

## EAGE PHOTO CONTEST 2008

In the past months we have received many truly wonderful entries to our photo contest. Now it is up to you to decide which photos are the very best.

**Come and see the ten best pictures during Rome 2008 in Hall 10, where the voting continues!**